Ionophores at work: Exploring the interaction of guanosine-based amphiphiles with phospholipid membranes

Giuseppe Vitiello,[a,b] Domenica Musumeci,[c] Alexandros Koutsioubas,[d] Luigi Paduano,[b,c] Daniela Montesarchio,[c,*] Gerardino D'Errico[b,c*]

[a]Department of Chemical, Materials and Production Engineering, University of Naples Federico II, Piazzale Tecchio 80, 80125 Naples, Italy.

[b]CSGI, Consorzio Interuniversitario per lo Sviluppo dei Sistemi a Grande Interfase, Via della Lastruccia 3, 50019 Sesto Fiorentino (Florence), Italy.

[c]Department of Chemical Sciences, University of Naples Federico II, Complesso Universitario di Monte S. Angelo, via Cintia 4, 80126 Naples, Italy.

[d]Jülich Centre for Neutron Science (JCNS) at Heinz Maier-Leibnitz Zentrum (MLZ), Forschungszentrum Jülich GmbH, Lichtenbergstr. 1, 85748 Garching, Germany.

*corresponding authors
e-mail: gerardino.derrico@unina.it Tel.: *+39 081 674245;* daniela.montesarchio@unina.it Tel.: *+39 081 674126*

Abstract

An amphiphilic derivative of guanosine, carrying a myristoyl group at the 5'-position and two methoxy(triethylene glycol) appendages at the 2' and 3'-positions (**1**), previously investigated as a synthetic ionophore, has been here studiedin its interaction mode with a model lipid membranealong with its 5'-spin-labelled analogue **2**,bearing the 5-doxyl-stearic in lieu of the myristic residue. Electron spin resonance spectra, carried out on the spin-labelled nucleolipid **2** in mixture with a DOPC/DOPG phospholipid bilayer, on one side, and on spin-labeledlipids mixed with **1,** on the other, integrated with dynamic light scattering and neutron reflectivity measurements, allowed ~~interpreting their functional behavior within biomembranes~~ and getting an in-depth picture of the effect of the ionophores on membrane structure, relevant for their ~~mechanism i their mechanism of action in~~ ion transport mechanism through lipid bilayers. Particularly, dehydration of lipid headgroups operated by the amphiphilic guanosines and insertion of the oligo(ethylene glycol) chains in the bilayer hydrophobic core have been found to play a fundamental role in driving the process, thus furnishingdirections to rationally implement future ionophores design.

Keywords: synthetic ionophores, guanosine derivatives, biomembranes, neutron reflectivity, electron spin resonance.

1. Introduction

Interaction with cell membranes is a crucial event for biologically active small organic molecules, which can be conveyed into the cell exploiting a variety of active or passive transport mechanisms [1,2]. Incidentally, the desired biological effects can be due also to the interaction with the membrane itself, e.g. as a result of targeting/inhibition of selected membrane proteins or of modification/destabilization of the membrane structure [3-5].

A classic example of the latter processes is provided by ionophores, i.e. synthetic amphiphiles able to transport cations or anions into the cells by forming specific channels or acting as carriers within the membrane bilayers [6-9]. By altering the ions concentration within the cytoplasm, these molecules can actively interfere with physiological processes or even reverse pathological effects (as in the case of chloride-transporting species, which could be able to compensate for the lack of chloride ions inside the cells of patients affected by channellopathies, such as cystic fibrosis [10,11]).

A variety of amphiphiles, based on very different backbones (e.g. peptides [12], crown ethers [13], carbohydrates [14], calixarenes [15], etc.), have been synthesized and analysed for their ion transport properties. Within this heterogeneous family, a mini-library of guanosine derivatives decorated on the ribose with various lipophilic and hydrophilic tethers has been also investigated [16,17]. Some of these derivatives proved to exhibit good ability to transport H^+ through phospholipid bilayers, as determined by the HPTS assay; in parallel experiments, poor selectivity for metal alkali cations but good selectivity for halogen anions emerged, with ionophoric activity increasing on going from the fluoride to the iodide, thus essentially following the lyotropic series. This ionophoric activity was accompanied by peculiar properties, i.e. antiproliferative activity against cancer cells and, in the presence of K^+ ions, ability to form stable superstructures stabilized by the guanine tetrads [16].

If guanine tetrad-based self-assembly did not seem to play a role in ion transport processes (indeed, no difference was detected in replacing Na^+ with K^+ ions in the used buffers, and the concentrations

investigated in the ion transport assays were far below those needed for G-quadruplex structuring), the presence of oligoethylene glycol chains on the ribose moiety proved to be an important structural motif, in analogy with previous results obtained by some of us on another class of synthetic ionophores, i.e. functionalized cyclic oligosaccharides (CyPLOS) derivatives [18-20].

Aiming at better elucidating the structure-activity relationships of this class of nucleolipids, in the search of indications for a rational design of second-generation guanosine-based ionophores, we here report studies on guanosine derivative **1** (Figure 1), carrying a myristoyl group at the 5'-position and two triethylene glycol appendages attached at the 2' and 3'-positions, and on its spin-labelled analogue (**2**, Scheme 1) mixed with dioleoylphosphocholine (DOPC)/dioleoylphosphoglycerol (DOPG) liposomes. To get a deeper insight into the interaction of these amphiphiles with model phospholipid bilayers, suitably mimicking cell membranes, electron spin resonance (ESR), dynamic light scattering (DLS) and neutron reflectivity (NR) studies have been exploitedin a combined approach to investigate - in both a qualitative and quantitative manner – the effects produced by these species.

2. Materials and methods

2.1. Materials

All the reagents were of the highest commercially available quality and were used as received. TLC analyses were carried out on silica gel plates from Merck (60, F254). Reaction products on TLC plates were visualized by UV light and then by treatment with a 10 % $Ce(SO_4)_2/H_2SO_4$ aqueous solution. For column chromatography, silica gel from Merck (Kieselgel 40, 0.063-0.200 mm) was used. NMR spectra were recorded on a Varian Inova 500 spectrometer, as specified. All the chemical shifts are expressed in ppm with respect to the residual solvent signal. Peak assignments were carried out on the basis of standard ^1H-^1H COSY and HSQC experiments. The following abbreviations were used to explain the multiplicities: s = singlet; d = doublet; t = triplet; q = quartet;

m = multiplet; b = broad; dd = double doublet. For the ESI MS analyses, a Waters Micromass ZQ instrument – equipped with an Electrospray source – was used in the positive mode.

Dichloromethane and methanol, HPLC-grade solvents, were obtained from Merck (Darmstadt, Germany), while the phospholipids 1,2-dioleoyl-sn-glycero-3-phosphocholine (DOPC) and 1,2-dioleoyl-sn-glycero-3-phosphoglycerol (DOPG) were obtained from Avanti Polar Lipids (Birmingham, AL, USA). PBS buffer (10 mM phosphate buffer, 137 mM NaCl, 2.7 mM KCl, pH 7.4) was obtained from Sigma-Aldrich (St. Louis, MO, USA). Spin-labeled phosphatidylcholines (n-PCSL, n = 5, 7, 10, 14) with the nitroxide group at different positions, n, in the sn-2 acyl chain were obtained from Sigma-Aldrich (St. Louis, MO, USA).The spin-labels were stored at -20°C in ethanol solutions at a concentration of 1 mg/mL.

2.2 Synthesis of guanosine derivative *2*

Guanosine derivative **1** (Figure 1) was synthesized as previously described [16].

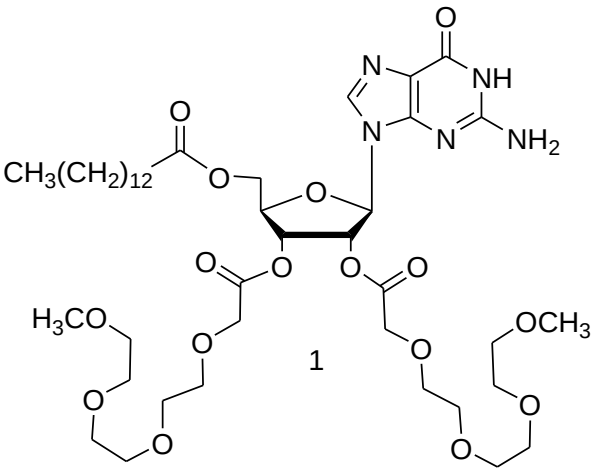

Figure **1.** Chemical structure of amphiphilic guanosine derivative **1**.

Guanosine analogue **2**, bearing a spin label on the lipophilic residue in 5'-position, was obtained starting from known derivative **3** [16], used as a valuablesynthetic precursor also in the preparation of **1**. Compound **3** was here coupled with 5-doxyl-stearic acid to give intermediate **4**, which was

then deprotected on the nucleobase yielding target derivative **2** by a simple treatment with 10% TFA in CH_2Cl_2, followed by repeated coevaporations from isopropanol till complete disappearance of excess TFA(Scheme 1).

All the products here synthesized were purified by silica gel column chromatography and then fully characterized by ^1H and ^{13}CNMR spectroscopy, as well as by ESI mass spectrometry.

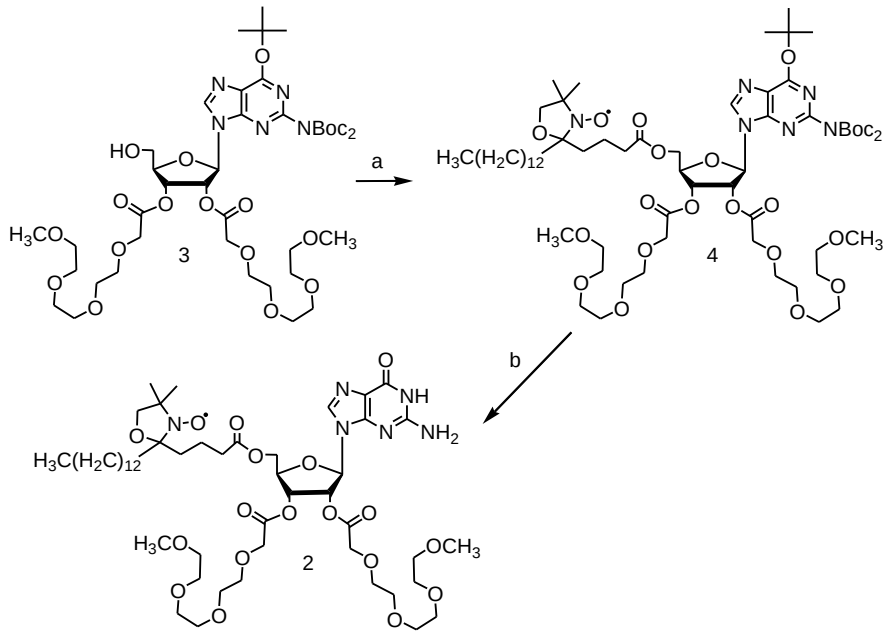

Scheme **1.** Synthesis of spin-labelled guanosine derivative **2**. Reaction conditions: a) 5-doxyl-stearic acid, DCC, DMAP, CH_2Cl_2, 3 h, r.t., quant.; b) 10% TFA in CH_2Cl_2, quant..

2.2.1. Synthesis of compound **4**

3 (7.0 mg, 0.0075 mmol), dissolved in 200 μL of anhydrous CH_2Cl_2, was reacted with DCC (2.9 mg, 0.014 mmol), DMAP (0.10 mg, 0.00070 mmol) and 5-doxyl-stearic acid (3.8 mg, 0.010 mmol) and the resulting mixture kept under stirring at room temperature. After 3 h the solvent was removed under reduced pressure and the residue purified on a silica gel column, eluted with acetone/n-hexane (1:1, v/v). The desired product **4** was obtained in almost quantitative yields (10 mg, 0.0070 mmol).

4: oil, R_f = 0.6 [acetone/n-hexane 3:2 (v/v)].

^{1}H NMR ($CDCl_3$, 500 MHz): relevant signals at δ 8.06 [s, 1H, H-8]; 6.16 [d, J = 5.0 Hz, 1H, H-1']; 5.94 [dd, J = 5.0 and J = 5.5 Hz, 1H, H-2']; 5.69 [bs, 1H, H-3']; 4.44 - 4.39 [overlapped signals, 3H, H-4', H-5'a and H-5'b]; 4.22 - 4.14 [overlapped signals, 4H, 2x -OCH_2CO-]; 3.74 - 3.64 [overlapped signals, 24H, 6x -OCH_2CH_2O-]; 3.54 [bs, 2H, -CH_2doxyl]; 3.38, 3.36 [overlapped singlets, 6H, 2x -OCH_3]; 2.40 – 2.35 [broad signals, 2H, CH_2-α stearic acid]; 1.95 - 1.84 [broad signals, 2H, CH_2-β stearic acid]; 1.71 [s, 18H, 2x -$OCOC(CH_3)_3$]; 1.58 [s, 9H, -$C(CH_3)_3$]; 1.48 - 1.23 [overlapped signals, 26H, 13x -CH_2-]; 1.17 - 1.10 [overlapped signals, 6H, 2x CH_3doxyl]; 0.87 [t, J = 6.5 and 6.5 Hz, 3H, -CH_3].

^{13}C NMR ($CDCl_3$, 100 MHz): relevant signals δ 168.9, 168.7 [3x -CO-]; 160.8 [C-6]; 151.5 [C-2]; 151.0 [C-4]; 150.3 [2x -O<u>C</u>$OC(CH_3)_3$]; 121.3 [C-5]; 86.4 [C-1']; 83.9 [C-4']; 82.7 [<u>C</u>$(CH_3)_3$]; 80.0 [2x -OCO<u>C</u>$(CH_3)_3$]; 73.6 [C-2']; 71.7 [C-3']; 71.1, 70.3 [6x -OCH_2CH_2O-]; 68.4, 67.8 [2x -O<u>C</u>H_2CO-, -<u>C</u>H_2CO-]; 63.4 [C-5']; 58.8 [2x -OCH_3]; 48.8 [CH_2COO-C5']; 33.6, 31.6, 30.3, 29.4, 29.0, 28.0, 27.8, 25.3, 24.6, 22.4 [14x -CH_2-, -$C(CH_3)_3$, 2x -$OCOC(CH_3)_3$, 2x CH_3doxyl]; 13.8 [CH_3].

ESI-MS (positive ions): calcd. for $C_{64}H_{109}N_6O_{22}$= 1313.7595; found m/z= 1314.40 [M + H^+]; 1336.44 [M + Na^+]; 1352.34 [M + K^+].

2.2.2. Synthesis of compound **2**.

4 (9.3 mg, 0.0070 mmol), dissolved in 225 μL of anhydrous CH_2Cl_2, was treated with 25 μL of TFA and the resulting solution was kept under stirring at room temperature. After 2.5 h the solvent was removed under vacuum and the crude coevaporated three times with isopropanol. The desired product **2** was thus obtained as a pure compound, not requiring further purification, in almost quantitative yields (7.4 mg, 0.0070 mmol).

2: amorphous solid, R_f = 0.3 [AcOEt/CH_3OH, 8:2 (v/v)].

^{1}H NMR ($CDCl_3$, 500 MHz): relevant signals at δ 8.12 - 8.06 [broad signals, 1H, H-8]; 6.19 - 6.07 [broad signals, 1H, H-1']; 6.07 – 6.02 [dd, J = 4.5 and 5.0 Hz, 1H, H-2']; 5.80 – 5.73 [broad signals,

1H, H-3']; 4.49 - 4.21 [broad signals, 5H, H-4', H_2-5', 2x -OCH_2CO-]; 3.75 - 3.47 [overlapped signals, 26H, 6x -OCH_2CH_2O-, -CH_2doxyl]; 3.37, 3.34 [singlets, 6H, 2x -OCH_3]; 2.50 - 2.35 [broad signals, 2H, CH_2-α stearic acid]; 1.86 - 1.67 [broad signals, 2H, CH_2-β stearic acid]; 1.61 - 1.02 [overlapped signals, 34H, 14x CH_2, 2x CH_3doxyl]; 0.96 - 0.88 [broad signals, 3H, -CH_3].

^{13}C NMR ($CDCl_3$, 100 MHz): relevant signals at δ 174.9 [-$CH_2\underline{C}O$-]; 171.8, 171.6 [2x -$OCH_2\underline{C}O$-]; 160.3 [C-6]; 140.3 [C-8]; 88.5 [C-1']; 81.9 [C-4']; 80.0, 79.9 [2x -$O\underline{C}OC(CH_3)_3$]; 75.0 [C-2']; 73.4 [C-3']; 72.5, 72.0 [6x -OCH_2CH_2O-]; 69.6 [2x -$O\underline{C}H_2CO$-]; 69.5 [-$\underline{C}H_2CO$-]; 64.5 [C-5']; 59.6 [2x -OCH_3]; 44.0 [-OCH_2- doxyl]; 35.2, 34.4, 33.6, 32.1, 31.2, 28.9, 25.4, 24.2, 20.4 [14x -CH_2-, -$C(CH_3)_3$, 2x -$OCOC(CH_3)_3$, 2x CH_3doxyl]; 14.9 [-CH_3].

ESI-MS (positive ion): calcd. for $C_{50}H_{85}N_6O_{18}$= 1057.5920; found m/z= 1059.91 [$M + H^+$]; 1094.86 [$M + K^+$].

2.3. Lipid samples preparation

For DLS and ESR experiments, liposomes of DOPC/DOPG (95:5 wt/wt) were prepared mixing appropriate amounts of DOPC and DOPG, dissolved in CH_2Cl_2–CH_3OH mixture (2:1 v/v, 10 mg/mL lipid concentration), in a round-bottom test tube. A thin lipid film was produced by evaporating the solvents with dry nitrogen gas. Final traces of solvents were removed by subjecting the sample to vacuum desiccation for at least 3 h. The samples were then hydrated with 400 μL of a buffered saline solution(HEPES 25 mM, 100 mM NaCl, pH 7 and repeatedly vortexed, obtaining a Multi-Lamellar Vesicles (MLVs) suspension, which was then extruded at room temperature (11 extrusions through a 100nm polycarbonate membrane) to obtain a Large Unilamellar Vesicles (LUVs) suspension. For the ionophore addition, the same procedure used for the measurements of the ionophoric activity was here adopted [16]. An aliquot of CH_3OH solution of the ionophore (8μL, 5mM) was added to the lipid suspension (final ionophore concentration 0.1mM) and the vial was incubated at 25 °C for 30 min. The sample was then investigated by DLS. For ESR measurements, 20μL of the sample was degassed by purging nitrogen, transferred into a 25 μL glass

capillary and immediately sealed. Two sets of ESR experiments were performed: in the former one, spin-labeled guanosine **2** was used and mixed with the lipid at the ionophore/lipid ratio ranged between about 1:99 and 10:90 in moles(i.e., between ~~5:95 and 50:50~~ 1:7 and 1:70 by weight); in the latter one, unlabeled guanosine **1** was used at a fixed 10:90 ionophore/lipid mole ratio, and the liposome composition included 1% by weight of one of the n-PCSL lipid probes.

For Neutron Reflectivity experiments, Supported Lipid Bilayers (SLBs) were prepared by vesicle fusion [21-23]: Small Unilamellar Vesicles (SUVs), of 25-35 nm in diameter, were formed by vortexing and sonicating for 3! 10 min the MLVs suspension obtained as described above. In this case, the ionophore **1** was included in liposome composition by adding a proper amount of its methanol solution to the lipid mixture before evaporation of the organic solvents, at a 10:90 mole ratio. The SUVs suspension (0.5 mg mL^{-1}) was injected into the NR cell, allowed to diffuse and adsorb to the silicon surfaces over a period of 30 min. The solid supports for neutron reflection were 8! 5! 1 cm^3 silicon single crystals cut to provide a surface along the (111) plane and pre-treated. After lipid adsorption the sample cell was rinsed once with deuterated water to remove excess lipid.

2.4. ESR measurements

ESR spectra were recorded with a 9 GHz Bruker Elexys E-500 spectrometer (Bruker, Rheinstetten, Germany). The capillaries were placed in a standard 4 mm quartz sample tube containing light silicone oil for thermal stability. All the measurements were performed at 25 °C. Spectra were recorded using the following instrumental settings: sweep width, 120 G; resolution, 1024 points; time constant, 20.48 ms; modulation frequency, 100 kHz; modulation amplitude, 1.0 G; incident power, 6.37 mW. Several scans, typically 64, were accumulated to improve the signal-to-noise ratio.

2.5. DLS measurements

DLS measurements were performed with a home-made instrument composed of a Photocor compact goniometer, a SMD 6000 Laser Quantum 50 mW light source operating at 5325 Å, a photomultiplier (PMT-120-OP/B) and a correlator (Flex02-01D) from Correlator.com. The experiments were carried out at the constant temperature (25.0 ± 0.1) °C, by using a thermostatic bath, and at the scattering angle θ of 90°. The scattered intensity correlation function was analyzed using a regularization algorithm [24]. The diffusion coefficient of each population of diffusing particles was calculated as the z-average of the diffusion coefficients of the corresponding distributions [25, 26]. Considering that the mixtures are dilute, the Stokes–Einstein equation could beused to evaluate the hydrodynamic radius, r_H, of the aggregates from their translation diffusion coefficient, D.

2.6. NR measurements

NR measurements were performed at (25.00 ± 0.05) °C on the MARIA of the Jülich Centre for Neutron Science at MLZ in Garching and D17 at the high flux reactor of the Institut Laue-Langevin (ILL) in Grenoble. MARIA is a vertical reflectometer [27], using temperature-regulated (through a connected Julabo F12-ED circulator) custom liquid cells. The design of the liquid cells is similar as the one used in a previous work [28]. The measurements were performed by varying the incidence angle of the incoming beam using two different wavelengths: 12 Å for the low-q region and 6 Å for the high-q region up to 0.20 $Å^{-1}$, with a wavelength spread $\Delta\lambda/\lambda = 0.1$. The D17 reflectometer was in the time of flight mode and the data were collected using neutrons with wavelengths in the range of 2–20Å at two incoming angles typically of 0.8° and 3.2°, resulting in a covered q range of 8! $10^{-3} Å^{-1} < q < 0.2$ $Å^{-1}$. The specular reflection at the silicon/water interface, R, defined as the ratio between the reflected and the incoming intensities of a neutron beam, is measured as a function of the wave vector transfer, q, perpendicular to the reflecting surface. R*(q)* is related to the scattering length density across the interface, $\rho(z)$, which depends on the composition of the adsorbed species. The neutron scattering length density, $\rho(z)$, is defined by the following equation:

$$\rho(z) = \Sigma_j n_j(z) b_j \quad (1)$$

where $n_j(z)$ is the number of nuclei per unit volume and b_j is the scattering length of nucleus j. Measurements were performed in aqueous medium containing a different amount of heavy water to increase the resolution in data analysis and reliability of the model used to describe the data [29]. The solid-liquid flow cells were connected to an HPLC pump to flush the solvents through the cells for solvent exchange. The pump was set at 2 mL/min speed and connected via switch to D_2O and H_2O reservoirs for the injection of pure D_2O (ρ = 6.35 ! 10^{-6} Å^{-2}); 4MW (ρ = 4 ! 10^{-6} Å^{-2}) which is a 66 % v/v D_2O – 34 % v/v H_2O mixture; Silicon Matched Water (SMW, ρ = 2.07 ! 10^{-6} Å^{-2}) which is a 32% v/v D_2O – 68% v/v H_2O mixture; and pure H_2O (ρ = -0.56 ! 10^{-6} Å^{-2}). Before the introduction of the lipid samples in the NR cells, the silicon blocks were characterized in terms of their native silicon oxide layer and of their surface roughness in three contrast solvents (D_2O, H_2O and SMW). Monocrystalline silicon blocks cut along the 111 direction were used as solid substrates. Ultra-polished Si blocks (dimensions 150! 50! 20mm^3) purchased from Andrea Holm GmbH were used as substrates and were cleaned before each experiment by soaking them in a 5:1:1 deionized water/29%, NH_4OH/30%, H_2O_2 solution maintained at 75 °C for 15min, followed by a rinse with milli-Q water. All of them were characterized prior to the NR experiment.

NR profiles were analyzed by box model fitting starting with simulations from the Aurore program [30]. The supported membrane is modelled as a series of boxes corresponding to the different bilayer regions. The program allows the simultaneous analysis of reflectivity profiles from the same sample in different contrast aqueous solutions, characterizing each box by its thickness, ρ, solvent volume fraction, and interfacial roughness. All the parameters were varied until the optimum fit to the data was found. The bare silicon substrate was characterized first in terms of thickness and roughness of the native oxide layer. The set of NR profiles was calculated for a uniform single layer model (the silicon oxide layer) of thickness 11 ± 1 Å, roughness 3 ± 1 Å and a scattering length

density of 3.41 ! 10^{-6} $Å^{-2}$, corresponding to 100% SiO_2. This step was followed by the characterization of the lipid bilayer.

3. Results

3.1. DLS analysis

DLS measurements were employed to investigate the fate of the amphiphilic guanosine **1** once added to an aqueous buffer in the absence or in the presence of DOPC/DOPG (95:5 wt/wt) liposomes, chosen as biomimetic membranes. This lipid composition is the same adopted for ion transport studies performed on **1** [16] and is designed to reproduce the distribution of anionic charges at the biomembrane interface [31]. Moreover, it allows a direct comparison with other studies previously carried out in our group on different ionophores [32]. Figure 2 shows that, in the aqueous medium, **1** tends to form micellar aggregates with an average diameter of about 15 nm. The samples have been monitored for one week and the aggregates have been found to be stable. A small population of larger aggregates ($r_H \approx 48$ nm) is also detectable. In the presence of DOPC/DOPG liposomes, the micelle population completely disappears, an evidence that the ionophore is completely solubilized by the lipid bilayer. At the same time, the liposome average dimension shifts only slightly to higher values (from about 95 nm to 105 nm), indicating that the aggregate morphology has not been perturbed by the guest molecule insertion.

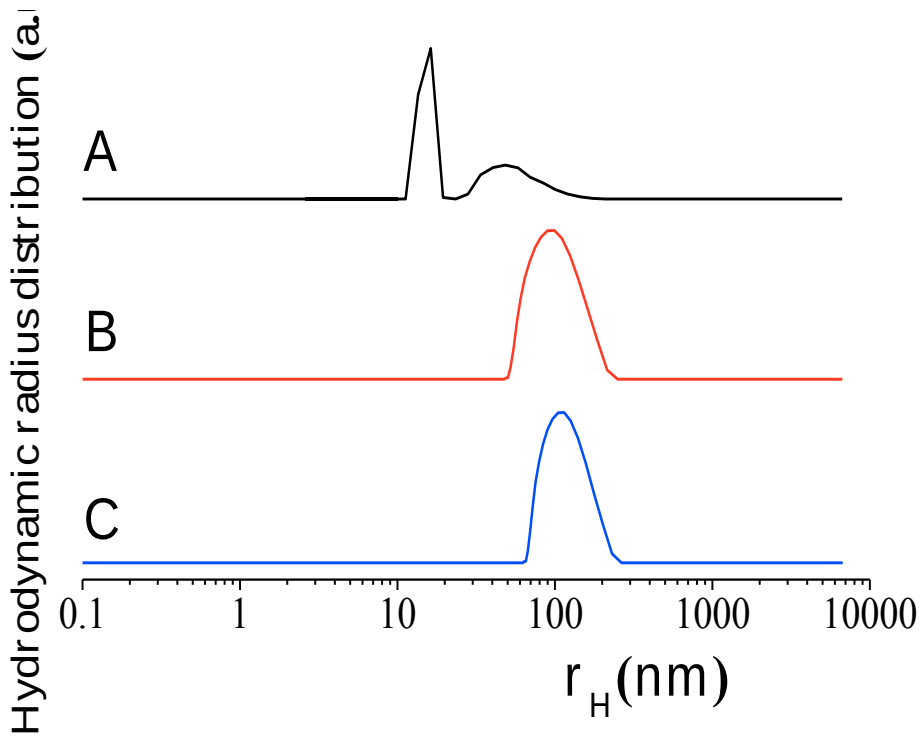

Figure **2** – Intensity weighed hydrodynamic radius distribution of aggregates of **1**(A), DOPC/DOPG liposomes before (B) and after (C) the addition of the guanosine based ionophore. The distributions were obtained from one of the DLS measurements performed with the instrumental configuration corresponding to a scattering angle of 90°.

3.2. ESR studies

ESR measurements were employed to investigate the interaction mode of guanosine-based amphiphiles**1** and **2**with biomembranes. Two sets of ESR experiments were performed. In the first one, spin-labeled **2**was used to directlymonitor the behavior of theguanosine-based ionophore in the presence of phospholipid bilayers. In the second set of measurements, spin-labeled phosphatidylcholines were included in the lipid membrane composition and the effects of the insertion of unlabeled **1** on their ESR spectra were analyzed.

In both cases, the same procedure adopted for ion transport measurements was used: an aliquot of the ionophore solution in methanol was added to theliposome suspension in buffer, havingfirst checked that methanol addition (2 % by volume with respect to the aqueous medium) did not alter

the liposome structure. The ESR spectrum of **2** in methanol presents a three-line shape with broad lines, typical of molecules freely (but relatively slowly) tumbling in solution, see Figure 3A. This evidence indicates that the ionophore does not self-aggregate in this solvent at the studied concentration. The quantitative analysis of this slow motion spectrum was realized by graphically estimating the isotropic nitrogen hyperfine coupling constant, a'_N, and the tumbling correlation time of the spin-probe, τ_C, according to the classical theory of motional narrowing of ESR lines [33,34]. These parameters provide information about the local physico-chemical properties of the label. In particular, a'_N depends on the polarity of the medium in which the nitroxide is embedded, whereas τ_C variations clearly show changes in the label rotational mobility, as determined by the microenvironment viscosity and/or by specific interactions. In particular, the apparent correlation time τ_C was determined according to [35]:

$$\tau_C = (0.65 \times 10^{-9})\, \Delta H_0 \left[(A_0/A_{-1})^{1/2} - 1\right] \qquad (2)$$

where ΔH_0 is the peak-to-peak width of the center line in Gauss, A_0 is the amplitude of the center line and A_{-1} is the amplitude of the high-field line. For the spectrum reported in Figure 3A, we obtained $a'_N = 14.50 \pm 0.02$ G and $\tau_C = (7.5 \pm 0.2) \times 10^{-10}$ s.

Once added to the liposome dispersion in buffer, the ionophore spectrum dramatically changes; Figures 3B-3E show the spectra of **2** registered in the presence of DOPC/DOPG bilayers at different guanosine/phospholipids ratios. A well-resolved anisotropic lineshape is observed in all cases, indicating that the rotational motion of the labelled molecules along one axis is different from that in the other two directions. This lineshape is typical of molecules associated to layered structures such as lipid bilayers, in which the rotation along the normal to the bilayer interface is different with respect to those along the axes lying on it. Thus, the ESR spectra clearly demonstrate that **2** associates with lipid bilayers, steadily inserting the hydrophobic tail within the lipid acyl chains.

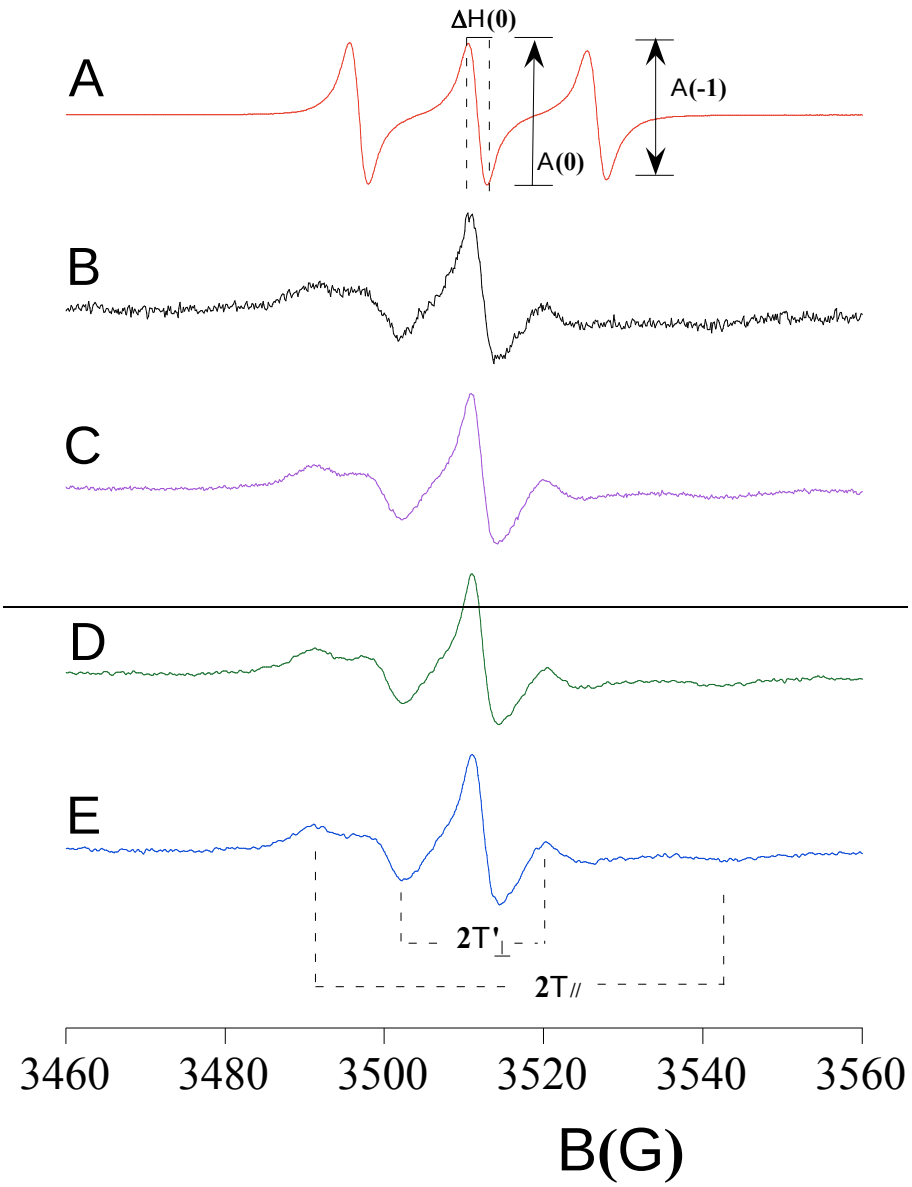
ΔH(0)
A
A(-1)
A(0)
B
C
D
E
2T'⊥
2T//
3460
3480
3500
3520
3540
3560
B(G)

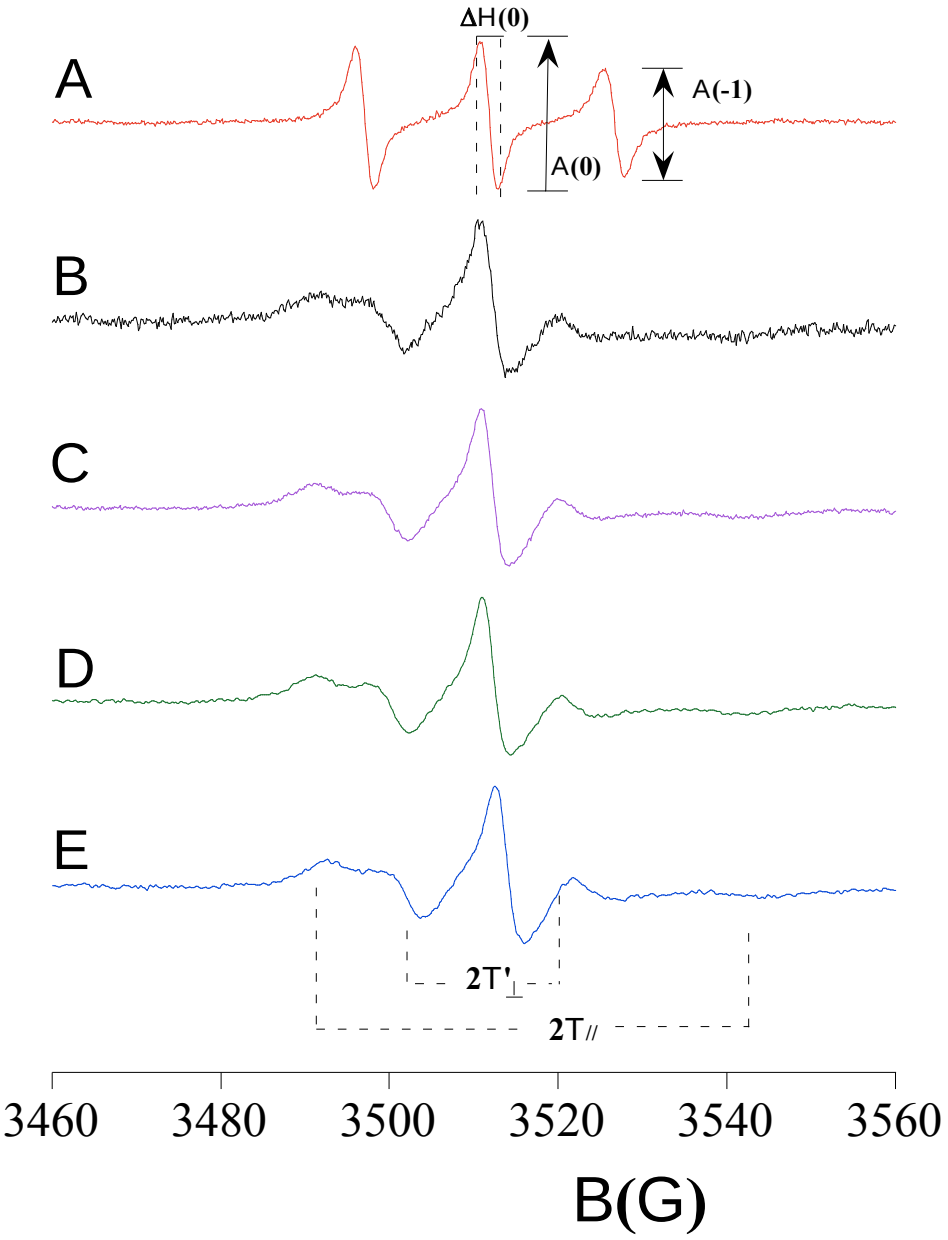

Figure 3 – ESR spectra of spin-labeled **2** in methanol (A) and DOPC/DOPG bilayers (B-E) at different **2**:phospholipid mole ratios i.e., in the order: 10:90, 5:95, 2:98, 1:99.

The absence of other superimposed signals demonstrates that the process is quantitative, since no "free" ionophore remains in the aqueous medium. Moreover, the absence of spin-exchange broadening of the spectra indicates that the paramagnetic labels do not interact among them, proving that ! " is molecularly dispersed among the lipid molecules, and does not form supramolecular structures embedded in the lipid bilayer (e.g., ion channels). A quantitative analysis of the spectra ? as performed by determining, from the splittings bet? een the minimum and

maximum points, the t? o phenomenological parameters a'_N and ! "@ABC ! is the order parameter and is related to the angular amplitudes of motion of the label, ? hich in turn reflects the motion of the acyl chain segment to ? hich the label is bound. a'_N and ! "? ere calculated according to the relationsD

$$a'_N = \frac{1}{3}\left(T_{\blacksquare} + 2T_{\perp}\right)$$

$$a'_N = \tfrac{1}{3}\,(T_{//} + T_{\perp}) \tag{3}$$

$$S = \frac{\left(T_{\blacksquare} - T_{\blacksquare}\right)}{\left(T_{zz} - T_{xx}\right)}\,\frac{a_N}{a'_N}$$

$$S = \frac{(T_{//} + T_{\perp})}{(T_{zz} + T_{xx})}\,\frac{a_N}{a'_N} \tag{4}$$

where $T_{\blacksquare}$ and $T_{\perp}$ are two phenomenological hyperfine splitting parameters which can be determined from the spectrum as shown in Figure 3 (note that $2T'_{\perp} = 2T_{\perp} - 1.6$). T_{xx} and T_{zz} are the principal elements of the real hyperfine splitting tensor in the spin Hamiltonian of the spin-label, which can be measured from the corresponding single-crystal EPR spectrum and are reported in the literature (T_{xx}=6.1 G and T_{zz}=32.4 G). a_N is the isotropic hyperfine coupling constant for the spin-label in crystal state, given by:

$$a_N = \frac{1}{3}\left(T_{zz} + 2T_{xx}\right) \tag{5}$$

The $\frac{a_N}{a'_N}$ ratio in equation (4) corrects the order parameter for polarity differences between the crystal state and the membrane. To obtain reliable values of the $T_{\blacksquare}$ and $T_{\perp}$ splittings, we adopted a home-made, MATLAB-based software routine. All values of the spectral parameters are collected in Table 1.

Table 1-The order parameter, ! , and the isotropic hyperfine coupling constant, a_N', of ! "in EFGHIEFGJ bilayers at different guanosine-based ionophore/phospholipid mole ratios.

Samples	S	a_N' /G
2:(DOPC/DOPG) 10:90	0.51 ± 0.02	14.8 ± 0.1
2:(DOPC/DOPG) 5:95	0.53 ± 0.02	15.0 ± 0.1
2:(DOPC/DOPG) 2:98	0.53 ± 0.02	15.0 ± 0.1
2:(DOPC/DOPG) 1:99	0.54 ± 0.02	15.1 ± 0.1

The ! and a_N' values are not affected by the 2/phospholipid ratio, supporting the idea that the ionophore is molecularly dispersed in monomeric form among the lipid molecules.

Hhanges in lipid supramolecular ordering and dynamics due to the interaction bet?een EFGHIEFGJ bilayers and the unlabeled guanosine-based ionophore **1** ?ere investigated by analyKingthe LMN spectra of phosphatidylcholines spin-labelled on the #"H-atom of the s#-Ochain (#-GHMP, # Q R, S, TU, TV) incorporated in the EFGHIEFGJ liposomes (TW by ?eight on total lipids). Xn the case of lipid bilayers in the liquid-crystalline (either disordered or ordered) state, the most probable localiKation of the nitroxide group corresponds to the fully extended conformation of the labelled acyl chain along the membrane normal, even though other conformations couldalso be present @S,AYC Honsequently, 5-PCSL, which bears the nitroxide reporter group close to the lipid hydrophilic headgroup, gives information on the acyl chain region just underneath the bilayer interface; on the contrary, 14-PCSL, which presents the nitroxide group positioned close to the acyl chain terminus, monitors the central region of the bilayer. 7-PCSL and 10-PCSL are representative of the intermediate segments of the acyl chains. The use of thesespin-labels in parallel allo?s a detailed analysis of perturbations of the different segments of the lipid hydrophobic tails. The spectra of n-PCSL in EFGHIEFGJ bilayers are shown in Figure 4. In the absence of **1** (continuous line), a flexibility gradient is evident in going from the 5-PCSL spectrum, which shows a clearly defined axially anisotropic lineshape, to the three-line, quasi-isotropic spectrum obtained for 14-PCSL.

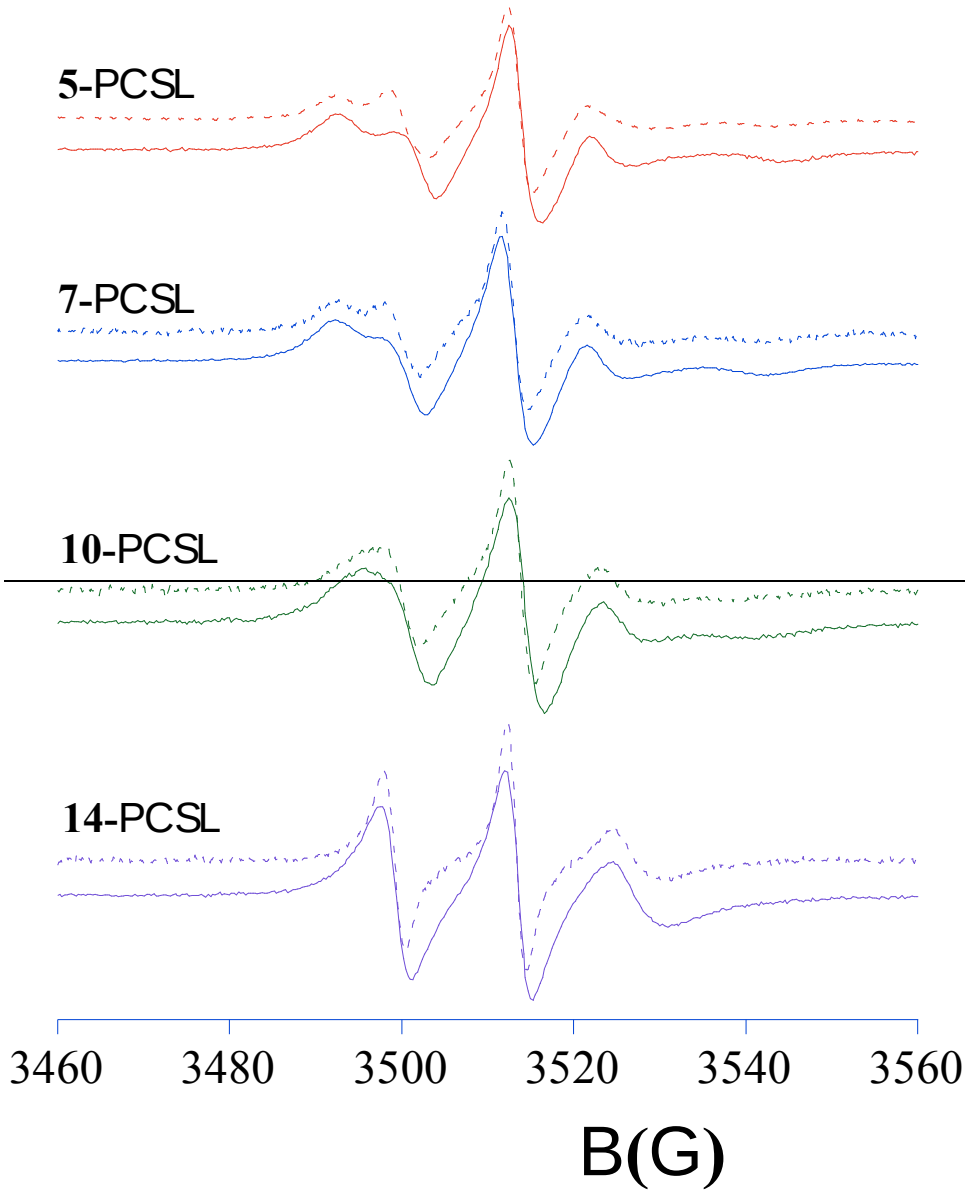
5-PCSL
7-PCSL
10-PCSL
14-PCSL
3460
3480
3500
3520
3540
3560
B(G)

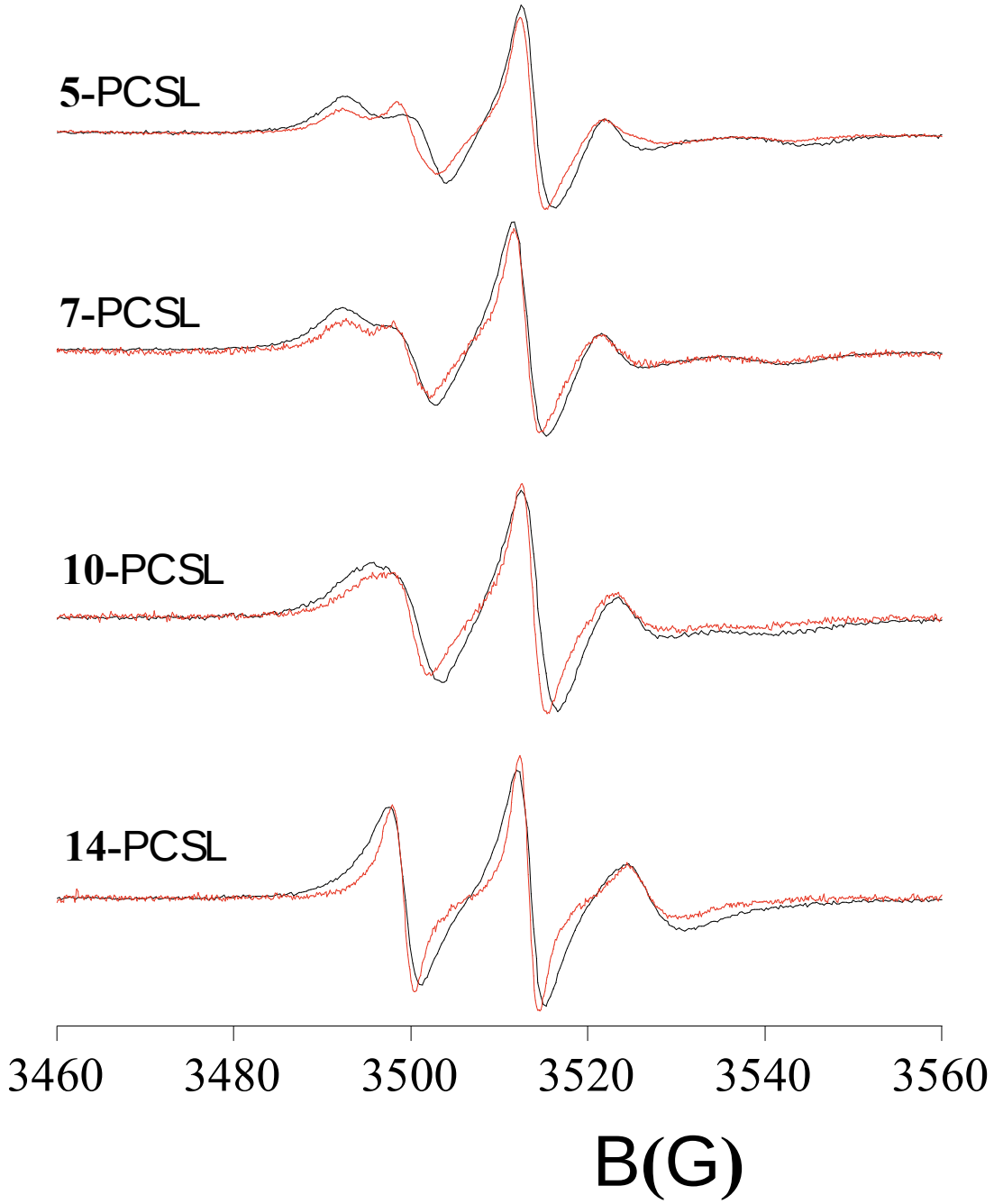

Figure **4** – ESR spectra of n-PCSL in DOPC/DOPG bilayers in the absence (black lines) and in the presence of **1** (10:90 mole ratio, red lines).

These evidences indicate an increase in segmental chain mobility experienced by the nitroxide group in going from the polar headgroups to the inner hydrophobic core, which is a characteristic hallmark of the liquid-crystalline state of fluid phospholipids bilayers @AZ,VUC Gerusal of [igure V reveals that, in the presence of #"(at a fixed 10:90 ionophore/lipid mole ratio), the flexibility

gradient is preserved, but the anisotropic behavior is significantly reduced for the phosphatidylcholines labeled at the R- and S- positions.

Particularly, addition of # to EFGHIEFGJ causes a clear decrease of !"at all # positions ([igure RA). At the same time, a_N' values also significantly decrease, indicating a reduction of the local polarity ([igure R\ ). These evidences indicate that insertion of #"into EFGHIEFGJ bilayers causes significant changes in the lipid pac]ing along the ?hole profile of the acyl chains, ?hich become less ordered^at the same time, polarity decreases (to a larger extent close to headgroups region).

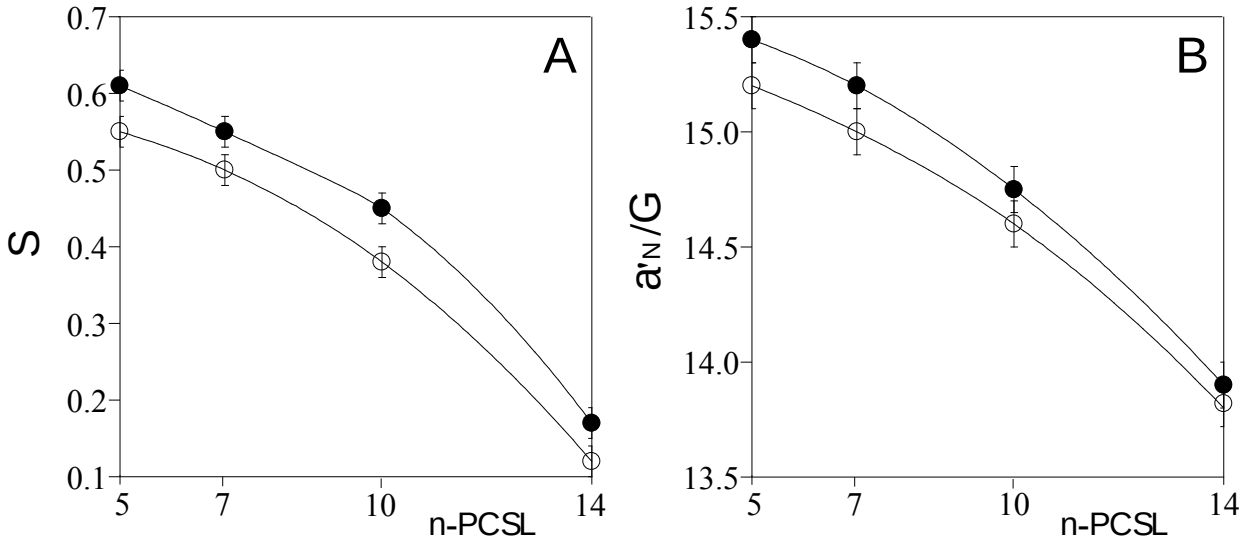

Figure **5** - Dependence on the nitroxide position along acyl chains, n, ~~guanosine-based amphiphile/lipid ratio~~ of the order parameter, S (panel A), and nitrogen hyperfine coupling constant, a_N' (panel B), of n-PCSL in pure DOPC/DOPG bilayers (close circles) and **1**:(DOPC/DOPG) bilayers (open circles) at fixed 10:90 ionophore/lipid mole ratio.

3.3. NR characterization

NR allows determining structure and composition of layers at interfaces. First, DOPC/DOPG supported bilayer in the absence of **1** was characterized by using D_2O, SMW and H_2O as isotopic contrast solvents. The experimental curves are shown in Figure 6A and the parameters used to fit the curves simultaneously from all the contrasts are given in Table 2. A five box model was found

to best fit the experimental curves. The first two boxes correspond to the silicon oxide and to the thin solvent layer interposed between the silicon surface and the adsorbed bilayer. The three other boxes describe the lipid bilayer, which is subdivided in the inner headgroups, the hydrophobic chains, and the outer headgroups layers. The theoretical scattering length densities, ρ, were calculated through equation (1). In the case of DOPC/DOPG 90:10 bilayer, ρ of the lipid headgroups is equal to 1.85! 10^{-6} Å^{-2} [41,42] while ρ of the acyl chains is equal to -0.21 ! 10^{-6} Å^{-2} [41]. These values were kept constant during the data analysis, since their optimization was found to give no fitting improvement. Thus, the parameters obtained from the best fit procedure are the thickness and the roughness of each box, plus the solvent content expressed as volume percent.

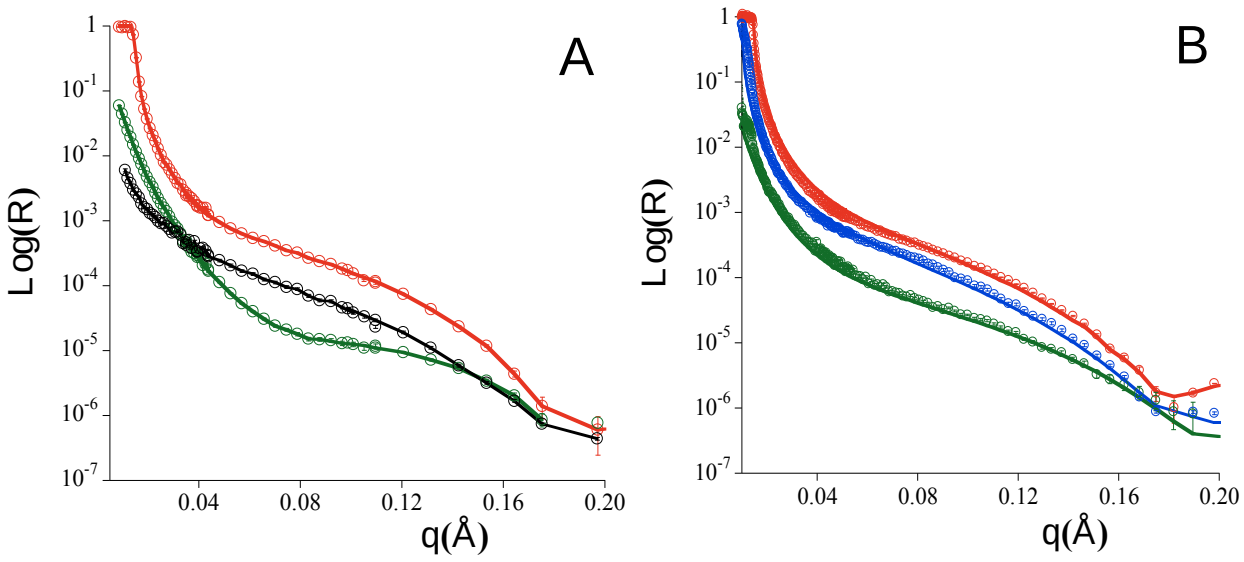

Figure **6** - Neutron reflectivity curves for lipid bilayers of DOPC/DOPG (panel A) and **1**:(DOPC/DOPG) (panel B) in D_2O (red), SMW (black), 4MW (blue) and H_2O (green) contrast solvents.

The values of all parameters optimized in curves fitting are reported in Table 2. Inspection of the table indicates that the overall bilayer thickness is about 42±1 Å and the roughness is low (~4 Å), while the solvent content is about 40% for both headgroup layers.

Table **2** - Parameters derived from model fitting the NR curves of DOPC/DOPG and **1**:(DOPC/DOPG) bilayers.

Lipid composition	interfacial layer	thickness (Å)	% solvent	roughness (Å)
DOPC/DOPG	water	3±1	100	3±1
	inner headgroups	7±1	40±10	4±1
	chains region	28±2	-	3±2
	outer headgroups	7±1	40±10	4±1
1:(DOPC/DOPG)	water	3±1	100	3±1
	inner headgroups	8±1	30±10	4±1
	chains region	31±2	-	3±2
	outer headgroups	11±1	30±10	4±1

The effect of the presence of **1** into DOPC/DOPG bilayers structure was also studied by acquiring the neutron reflectivity curves using D_2O, 4MW and H_2O as isotopic contrast solvents, as shown in Figure 6B. Also in this case, a five box model was found to best fit the experimental curves, but a good curve fitting was obtained varying the parameters related to the hydrophobic and hydrophilic layers (Table 2). In addition, the overall thickness (equal to 51±1 Å) increases of ~9 Å, confirming the insertion of guanosine-based ionophore into the DOPC/DOPG bilayer. In particular, changes were mainly observed in the hydrophilic layers: ρ increases to a value of ~2.1 ! 10^{-6} Å^{-2}, clearly indicating the presence of molecules of **1** into the lipid membrane. Particularly, the thickness increasesby ~2 and ~3 Å for the inner and outer headgroup layers, respectively, while the hydrophobic region thickness increases of ~3 Å. Remarkably, a decrease in the solvent content of the external headgroup layer was also obtained. No significant change was detected in the roughness of the whole bilayer. This model suggests that the guanosine-based amphiphile stably interacts with the biomembranes (see scattering length density profiles in Figure 7), partially modifying the lipids organization and increasing both its ~~compactness and~~ thickness.

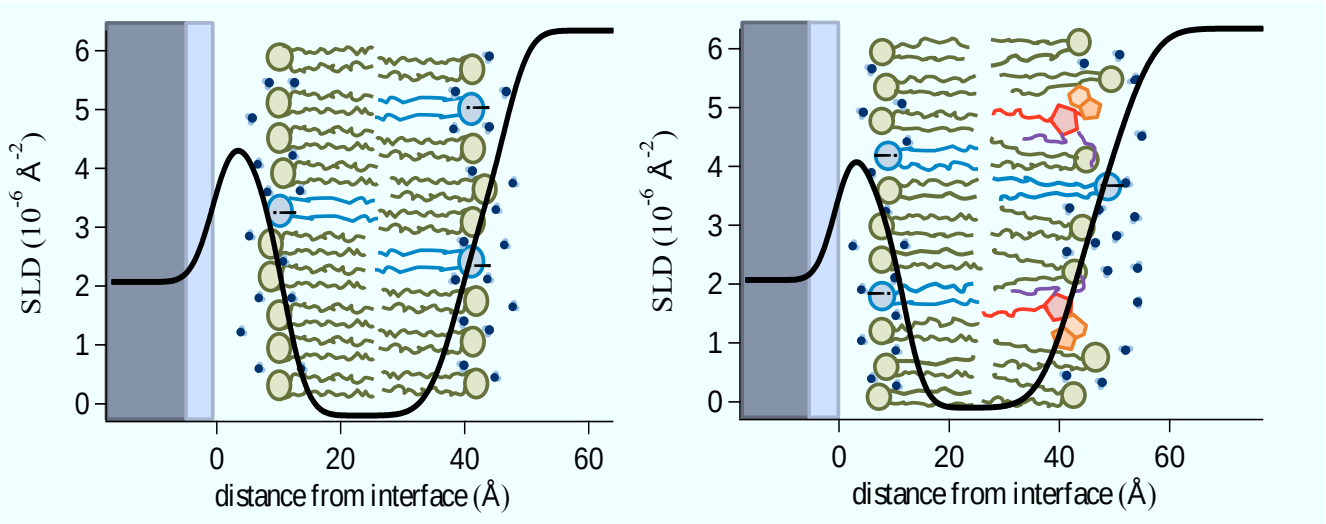

Figure 7– Scattering Length Density (SLD) profiles in D_2O for lipid bilayers of DOPC/DOPG (on the right) and **1**:(DOPC/DOPG) (on the left).

4. Discussion

Amphiphilicguanosines have been shown to be active ionophores. The promising ion transportation resultshave beeninterpreted as due to the membranotropic attitude of these molecules, and to their effects on the lipid bilayer [16,17]. However, a molecular description of the ionophore/membrane interaction is still lacking. In the present work we analyze how one representative amphiphilic guanosine, **1**, interacts with bilayers formed by the zwitterionic lipid DOPC and the anionic lipid DOPG in a 95:5 weight ratio. DOPC/DOPG bilayers are designed to reproduce the partial negative charge of biomembranes. At room temperature they present a fluid liquid crystalline arrangement of the acyl tails similar to that of cholesterol-poor domains of eukaryotic biomembranes. **1** is a guanosine derivative presenting a saturated fatty acid residue, that is myristic acid, attached to the 5'-OH group of ribose, and two monomethoxytriethyleneglycol (methoxy-TEG) groups attached to the secondary hydroxyl groups. Schematically, **1** can be considered as a central ribose unit with four appendages, whose different solvent preferences determine the amphiphilic behavior of the whole molecule. The myristoyl moiety presents an obvious lipophilic character; on the other hand, the oligo(ethylene glycol) chains tend to be strongly hydrated, even though their hydrophilicity is finely regulated by local concentration [43] and temperature [44]. The guanine solvophilic behavior is

complex being determined by the concomitant presence of aromatic rings and multiple sites available for H-bonding. Both experiments and calculations show that guanine is quite hydrophilic, with a low chloroform/water partition coefficient, but in aqueous solution presents a strong tendency to oligomerize by π–π stacking interactions [45].

The amphiphilic behavior of **1** drives its micellization in aqueous solution, as highlighted by DLS experiments. In the presence of liposomes, thesemicelles disappear, and **1** is completely solubilized by the lipid bilayer. Liposomes include these guest molecules without markedchanges in their morphology, evidence that local bilayer perturbations do not lead to dramatic lipid rearrangement. The high membranotropic attitude of **1** demonstrates its optimal molecular design and the correct balance between hydrophobic and hydrophilic moieties.

The interaction mode of **1** with DOPC/DOPG bilayers has been investigated at the molecular level by combining ESR and NR data. ESR spectroscopy, by a skillful use of spin-labels, has been demonstrated to be extremely informative on the interaction of guest molecules with lipid membranes. The guests and the lipids can be alternatively labelled, thus allowing a complete and detailed analysis of the system structure and behavior. To have a direct insight into the mechanism of action of **1**, spin-labelled analogue **2**- carrying a stable nitroxide group in position 5 of the saturated acyl chain - has been purposely designed and synthesized. Thespectra of **2** confirm that amphiphilic guanosines quantitatively solubilize in the lipid bilayer. No evidence of ionophore self-aggregation within the membrane is detected, thus ruling out the formation of supramolecular assemblies acting as ion channels. Davis and co-workers reported the formation of well-structured channels constituted by stacked assembliesof guanine tetrads; however, in this case the guanosine units were covalently linked so to form a rigid unimolecular scaffold promoting their correct organization [46]. In following studies, guanosines supramolecular organization was promoted by their conjugation with bis-urea [47] or bis-carbamate linkers [48]. Our results show that,under the studied concentration conditions, hydrogen bonding among guanines, and the following stacking among the resulting guanine tetrads to give G-quadruplex structures are not realized, thus excluding

possible guanosine self-assembly in membranes.

! "and the #-GHMP spin-labelled lipids carry exactly the same label(a doxyl paramagnetic ring). This allows a direct comparison between the a'_N value obtained for ! in DOPC/DOPG bilayers (≈ 15 G)and those obtained for n-PCSL in the same membrane (see Figure 6B), by applying a sort of "molecular ruler approach" [49]; it appears that position 5 of the myristoyl chain of **2** is positioned at the same level of position 7 of the lipids. Thus, the experimental results point to the insertion of the ionophore hydrophobic tail among the acyl chains of the lipids, the ribose unit being positioned slightly below the membrane hydrophilic interphase. This is consistent with the insertion of the guanine moiety among the lipid headgroups. This is likely the optimal positioningfor guanine, which can form H-bonds with the oxygens of the phosphate groups. This behavior could closely resemble that of tryptophan, an aminoacid with a bicyclic aromatic skeleton and H-bonding ability, which presents a well-assessed attitude to position itself at the interphases [50,~~40~~, 51].

Because of the ribose positioning relatively deep into the lipid bilayer, methoxy-TEG chains are shielded from complete exposure to the aqueous medium. Rather, they either remain embedded within lipid headgroups or inserted into the bilayer hydrophobic core. Both locations are possible as a result of a peculiar property of polyethylene glycol chains: at a high degree of hydration theseare hydrophilic, while at a low degree of hydration they assume a hydrophobic behavior [~~51~~ 52]. The energy barrier for the polyethylene glycol penetration into the lipid bilayer is quite lo? and can be easily overcome ? henits chain termini are capped ? ith hydrophobic groups [~~52~~ 51]. **1** and **2** present TEG chains whose terminal hydroxyls have been masked as methyl ethers, so that they can be dehydrated at the membrane interphase and/or transported into the lipid bilayer. ESR data show that interaction of **1** with DOPC/DOPG membranescauses a reduction of lipid ordering. This indicates an at least partial insertion of the methoxy-TEG chains among the lipid acyl chains [32]. It has to be noted that disordering of the lipid tails cannot be due to the insertion of the myristoyl chain, which is completely saturated and should lead to an opposite effect [53]. At the same time, both ESR and

NR data show that the ionophore insertion into the lipid bilayer causes a decrease of the local hydration of the membrane interface. Specifically, the water content in the headgroup region drops from 40 to 30 %by volume, and this reflects in a significant lowering of the $a_N^{'}$ value. Thus, the experimental data support the hypothesis that dehydrated methoxy-TEG chains could concur to replace, along with guanines, water molecules hydrating lipid headgroups. The presence of these bulky groups causes an increase of the thickness of the headgroup layer, as detected by NR.

Reduction of headgroup hydration likely plays a fundamental role in the action mechanism of the ionophore, similarlytoother guest molecules involved in important biological processes.Indeed, recent simulations have shown that perturbation of the aqueous layer near the membrane is the first step of the translocation of an anionic DNA fragment through a lipid membrane, followed by local de-hydration [54]. The hydration structure of lipid headgroups determines the interfacial curvature of the amphiphilic aggregates [55,56] and has been proposed to control the dynamics of membrane processes involving changes in lipid supramolecular organization (e.g., membrane fusion [57,40]). On this basis, dehydration of the lipid headgroups can be proposed to play a synergistic role, with methoxy-TEG insertion causing a significant decrease of the lipid ordering along the whole bilayer profileupon insertion of **1**.

Taken together, the experimental evidences presented in this work indicate that the ionophoric activity exerted by amphiphilicguanosines is an indirect effect of their interaction with lipid bilayers, resulting in lipid tails disordering and membrane dehydration. Lipid disordering is a common feature of ionophores whose mechanism of action is based neither on ion channels formation, nor on ion complexation by specific carriers. As an example, the ionophoric activity of CyPLOS derivatives has been found to be related to the formation of a disordered zone in the membrane characterized by an increased ion-permeability [32]. Another common aspect of the ionophoric machinery is the altered hydration of the membrane interphase. Ion selectivity tests have shown that the transportation process is governed by the translocation of the anion and in particular

limited by the cost of its dehydration. The results reported in the present work clearly suggest that amphiphilic guanosines, when inserted into phospholipid bilayers, following mechanisms similar to those observed for lipid headgroup de-hydration, are able to lower this cost or the energetic barriers of the ion de-hydration process, thus favoring the ion transportation process across membranes.

Conclusions

This study has been aimed at the comprehension of the molecular mechanisms underlying the ion transport across biomembranes operated by the amphiphilic guanosines **1** and **2**, as a necessary prerequisite for the design of novel, optimized bioactive compounds. The obtained data indicate that lipid membrane permeabilization is a consequence of the bilayer perturbation due to the ionophore interaction. Amphiphilic guanosines are solubilized in unimeric form by the lipid bilayer, in no case producing ion channels or other ionophores super-aggregates. On the other hand, the integrity of the lipid membrane is preserved. Once included in the bilayer, the ionophore positions itself close to the boundary between the hydrophobic and hydrophilic regions of the bilayer, with the hydrophobic chain inserted among the lipid acyl chains, and the guanine anchored to the lipid headgroups. In this situation, de-hydrated methoxy-TEG moieties either penetrate within the lipid tails, disturbing their packing, or remain embedded within the lipid headgroups, replacing water molecules. Lipid disordering and bilayer interphase de-hydration finally result in the local membrane destabilization, which favors ion translocation. Taking into account that guanosine-based amphiphiles such as **1** and related analogues show largely and finely tunable properties as a function of the nature of the ribose substituents, optimization of the ionophore activity of these nucleolipids can be easily expected from suitable design modifications of **1**, e.g. from replacement of the myristoyl moiety with longer chainsor other lipids (e.g., similar to cholesterol) to further increase the ionophore solubilization into the bilayer, substitution of guanine with other aromatic groups with higher H-bonding ability (e.g., hydroxyguanine) to strengthen the interaction with the lipid headgroups, and elongation of the oligo(ethyleneglycol) chains to enhance lipid disordering and headgroup de-hydration. Based on the

acquired knowledge, further studies are thus currently in progress for the design and synthesis of a second generation of amphiphilic guanosines, with enhanced biological/biomedical potential.

Acknowledgements.

This work was supported by the Italian Association for Cancer Research (AIRC) (IG2015 n. 17037 to D.M.). G.V. and L.P. thanks the Heinz Maier- Leibnitz Zentrum (MLZ) and Institut Laue-Langevin (ILL) for awarding neutron beam-time.

Abbreviations

AcOEt = ethyl acetate; Boc = tert-butoxycarbonyl; DCC = N,N-dicyclohexylcarbodiimide; DLS = Dynamic Light Scattering; DMAP = 4-dimethylaminopyridine;DOPC = 1,2-dioleoyl-sn-glycero-3-phosphocholine; DOPG = 1,2-dioleoyl-sn-glycero-3-phosphoglycerol; ESR = Electron Spin Resonance; HEPES = 4-(2-hydroxyethyl)-1-piperazineethanesulfonic acid; LMV = Large MultilamellarVescicles; LUV= Large UnilamellarVescicles;MLV = Multilamellar Vesicles; NR = Neutron Reflectivity; PBS = phosphate-buffered saline; n-PCSL = phosphatidylcholine spin label positional isomers; SLB = Supported Lipid Bilayers; SUV = Small UnilamellarVescicles; TFA = trifluoroacetic acid.

References

1. M.V. LeVine, M.A. Cuendet, G. Khelashvili, H. Weinstein. Allosteric Mechanisms of molecular machines at the membrane: transport by sodium-coupled symporters. Chem. Rev. 116 (2016) 6552-6587.
2. H. Canton, G. Battaglia. Endocytosis at the nanoscale. Chem. Soc. Rev. 41 (2012) 2718-2739.
3. C. Pliotas, J. H. Naismith. Spectator no more, the role of the membrane in regulating ion channel function. Curr. Opin. Struct. Biol. 45 (2016)59-66.
4. A. I. Herrera, J. M. Tomich, O. Prakash. Membrane interacting peptides: A Review. Curr. Protein Pept. Sci. 17 (2016) 827-841.
5. H. Tsuchiya. Membrane interactions of phytochemicals as their molecular mechanism applicable to the discovery of drug leads from plants. Molecules 20 (2015) 18923-18966.
6. P. Subramanyam, H. M. Colecraft. Ion channel engineering: perspectives and strategies.J. Mol. Biol. 427 (2015) 190-204.
7. F. De Riccardis, I. Izzo, D. Montesarchio, P. Tecilla. Ion transport through lipid bilayers by synthetic ionophores: modulation of activity and selectivity. Acc. Chem. Res. 46 (2013) 2781-2790.
8. G. W. Gokel, S. Negin. Synthetic ion channels: from pores to biological applications.Acc. Chem. Res. 46 (2013)2824-2833.
9. T. M. Fyles. Synthetic ion channels in bilayer membranes.Chem. Soc. Rev. 36 (2007) 335-347.
10. M. A. Kamaleddin. Molecular, biophysical, and pharmacological properties of calcium-activated chloride channels.J. Cell. Physiol. 2017 Jan 25. doi: 10.1002/jcp.25823.
11. R.I. Planells-Cases, T.J. Jentsch. Chloride channelopathies. Biochim. Biophys. Acta. 1792 (2009) 173-189.

12. F. Otis, M. Auger, N. Voyer. Exploiting peptide nanostructures to construct functional artificial ion channels.Acc. Chem. Res. 46 (2013) 2934–2943.
13. G. W. Gokel,S: Negin. Synthetic membrane active amphiphiles. Adv. Drug Deliv. Rev. 64 (2012)784-796.
14. D. Montesarchio, C. Coppola, M. Boccalon, P. Tecilla. Carbohydrate-based synthetic ion transporters. Carbohydr. Res. 356 (2012) 62-74.
15. L. Mutihac. Functionalized calix[n]arenes as membrane transporters for biological compounds. A minireview. Curr. Drug Discov. Technol. 5 (2008) 98-104.
16. L. Simeone, D. Milano, L. De Napoli, C. Irace, A. Di Pascale, M. Boccalon, P. Tecilla, D: Montesarchio. Design, synthesis and characterisation of guanosine-based amphiphiles. Chem. Eur. J.17 (2011) 13854-13865.
17. D. Musumeci, C. Irace, R. Santamaria, D. Milano, P. Tecilla, D. Montesarchio. Guanine-based amphiphiles: synthesis, ion transport properties and biological activity. Bioorg. Med. Chem. 23 (2015) 1149–1156.
18. C. Coppola, A. Paciello, G. Mangiapia, S. Licen, M. Boccalon, L. De Napoli, L.Paduano, P. Tecilla, D. Montesarchio. Design, synthesis and characterisation of a fluorescently labeled CyPLOS ionophore. Chem. Eur. J.16 (2010) 13757-13772.
19. S. Licen, C. Coppola, J. D'Onofrio, D. Montesarchio, P. Tecilla. CyPLOS: a new family of synthetic ionophores. Org. Biomol. Chem. 7 (2009) 1060-1063.
20. C. Coppola, V. Saggiomo, G. Di Fabio, L. De Napoli, D. Montesarchio. Novel amphiphilic cyclic oligosaccharides: synthesis and self-aggregation properties. J. Org. Chem. 72 (2007) 9679-9689.
21. G. Vitiello, G. Fragneto, A. A. Petruk, A. Falanga, S. Galdiero, A. M. D'Ursi, A. Merlino, G. D'Errico. Cholesterol modulates the fusogenic activity of a membranotropic domain of the FIV glycoprotein gp36. Soft Matter 9 (2013)6442–" #$" .

22. G. Vitiello, A. Falanga, A. A. Petruk, A. Merlino, G. Fragneto, L. Paduano, S. Galdiero, G. D'Errico. Fusion of raft-like lipid bilayers operated by a membranotropic domain of the HSV-type I glycoprotein gH occurs through a cholesterol dependent mechanism. Soft Matter 11 (2015) 3003–%&' " .
23. G. Vitiello, A. Luchini, G. D'Errico, R. Santamaria, A. Capuozzo, C. Irace, D. Montesarchio, L. Paduano. Cationic liposomes as efficient nanocarriers for the drug delivery of an anticancer cholesterol-based ruthenium complex. J. Mater. Chem. B 3 (2015) 3011–3023.
24. A. Lomakin, D.B. Teplow, G.B. Benedek, Quasielastic light scattering for protein assembly studies, in: E.M. Sigurdsson (Ed.), Amyloid proteins: methods and protocols, vol. 299, Humana Press, Totowa, New Jearsey, 2005.
25. H.X. Zhang, O. Annunziata, Effect of macromolecular polydispersity on diffusion coefficients measured by Rayleigh interferometry, J. Phys. Chem. B 112 (2008) 3633–3643.
26. A. Luchini, C. Irace, R. Santamaria, D. Montesarchio, R. K. Heenan, N. Szekely, A. Flori, L. Menichetti, L. Paduano, Phosphocholine-decorated superparamagnetic iron oxide nanoparticles: defining the structure and probing in vivo applications. Nanoscale 8 (2016) 10078-10086.
27. S. Mattauch, A. Koutsioubas, S. Putter, MARIA: Magnetic Reflectometer with high Incident Angle. Journal of large-scale research facilities 1 (2015) A8.
28. A. Koutsioubas, Combined Coarse-Grained Molecular Dynamics and Neutron Reflectivity Characterization of Supported Lipid Membranes. J. Phys. Chem. B, 120 (2016), 11474-11483.
29. G. Fragneto, R. K. Thomas, A. R. Rennie, J. Penfold. Neutron reflection from hexadecyltrimethylammonium bromide adsorbed on smooth and rough silicon surfaces. Langmuir 12(1996) 6036–6043.

30. A. Nelson, Co-refinement of multiple-contrast neutron/X-ray reflectivity data using MOTOFIT. J. Appl. Crystallogr., 39 (2006) 273-276.
31. G. D'Errico, G. Vitiello, O. Ortona, A. Tedeschi, A. Ramunno, A. M. D'Ursi. Interaction between Alzheimer's Aβ(25–35) peptide and phospholipid bilayers: the role of cholesterol. Biochim. Biophys. Acta 1778 (2008) 2710–2716.
32. E. Busi, G. Vitiello, M. Niccoli, R. Basosi, D. Montesarchio, G. D'Errico. On the mechanism of ion transport through lipid membranes mediated by PEGylated cyclic oligosaccharides (CyPLOS): An ESR study. Biochim. Biophys. Acta 1828 (2013) 2074–2082.
33. D. Kivelson. Theory of ESR linewidths of free radicals. J. Chem. Phys. 33 (1960) 1094–1106
34. G. Vitiello, M. Grimaldi, A. Ramunno, O. Ortona, G. De Martino, A. M. D'Ursi, G. D'Errico, Interaction of a β-sheetbreaker peptide with lipidmembranes. J. Pept. Sci. 16 (2010) 115–122.
35. I. R. Bates, J. M. Boggs, J. B. Feix, G. Harauz, Membrane-anchoring and charge effects in the interaction of myelin basic protein with lipid bilayers studied by site-directed spin labelling. J. Biol. Chem. 278 (2003) 29041–29047.
36. S. Galdiero, A. Falanga, G. Vitiello, M. Vitiello, C. Pedone, G. D'Errico, M. Galdiero. Role of membranotropic sequences from herpes simplex virus type I glycoproteins B and H in the fusion process. Biochim. Biophys. Acta 1798 (2010) 579–591.
37. A. Vogel, H.A. Scheidt, D. Huster, The distribution of lipid attached spin probes in bilayers: application to membrane protein topology, Biophys. J. 85 (2003) 1691–1701.
38. B. Dzikovski, V. Livshits, J. Freed, Sphingomyelin/phosphatidylcholine/cholesterol phase diagram: boundaries and composition of lipid rafts, J. Phys. Chem. B 119 (2015) 13330–13346.

39. G. Vitiello, A. Falanga, M. Galdiero, D. Marsh, S. Galdiero, G. D'Errico. Lipid composition modulates the interaction of peptidesderiving from herpes simplex virus type i glycoproteins B and H with biomembranes, Biochim. Biophys. Acta1808 (2011) 2517–2526.

40. A. Merlino, G. Vitiello, M. Grimaldi, F. Sica, E. Busi, R. Basosi, A. M. D'Ursi, G. Fragneto, L. Paduano, G. D'Errico, Destabilization of lipid membranes by a peptide derived from glycoprotein gp36 of feline immunodeficiency virus: a combined molecular dynamics/experimental study, J. Phys. Chem. B 116 (2012) 401–412.

41. H. P. Vacklin, F. Tiberg, R.K. Thomas, Formation of supported phospholipid bilayers via co-adsorption with β-d-dodecylmaltoside. Biochim. Biophys. Acta 1668(2005) 17–24.

42. A. Luchini, Y. Gerelli, G. Fragneto, T. Nylander, G. K. Pálsson, M.-S. Appavou, L. Paduano, Neutron Reflectometry reveals the interaction between functionalized SPIONs and the surface of lipidbilayers. Colloids Surf. B 151(2017) 76-87.

43. L. Ambrosone, G. D'Errico, R. Sartorio, L. Costantino, Dynamic properties of aqueous solutions of ethylene glycol oligomers as measured by the pulsed gradient spin-echo NMR technique at25 °C.J. Chem. Soc., Faraday Trans.93 (1997) 3961–3966.

44. M. J.Hey, S. M. Ilett, G. Davidson,Effect of temperature on poly(ethyleneoxide) chains in aqueous solution. A viscometric, ^{1}H NMR and Ramanspectroscopicstudy, J. Chem. Soc., Faraday Trans.91 (1995) 3897–3900.

45. R. F. Ribeiro, A. V. Marenich, C. J.Cramer, D. G. Truhlar, The solvation, partitioning, hydrogen bonding, and dimerization of nucleotide bases: a multifaceted challenge for quantum chemistry, Phys. Chem. Chem. Phys. 13 (2011) 10908–10922.

46. M. S. Kaucher, W. A. Harrell, J. T. Davis, A unimolecular G-quadruplex that functions as a synthetic transmembrane Na^{+} transporter, J. Am. Chem. Soc. 128 (2006) 38–39.

47. L. Ma, M. Melegari, M. Colombini, J. T. Davis, Large and stable transmembrane pores from guanosine−bile acid conjugates, J. Am. Chem. Soc.130 (2008) 2938–2939.

48. L. Ma, W. A. Harrell, J. T. Davis, Stabilizing guanosine-sterol ion channels with a carbamate to urea modification in the linker, Org. Lett. 11 (2009) 1599–1602.

49. M. Bortolus, A. Dalzini, F. Formaggio, C. Toniolo, M. Gobbo, A. L. Maniero, An EPR study of ampullosporin A, a medium-length peptaibiotic, in bicelles and vesicles, Phys. Chem. Chem. Phys.18 (2016) 749–760.

50. W. C.Yau, W. C.Wimley, K.Gawrisch, S. H.White, The preference of tryptophan for membrane interfaces, Biochemistry 37 (1998) 14713–14718.

51. G. Liu, L. Fu, G. Zhang, Role of hydrophobic interactions in the adsorption of poly(ethyleneglycol) chains on phospholipid membranes investigated with a quartz crystal microbalance, J. Phys. Chem. B, 113 (2009) 3365–3369.

52. S. Pal, G. Milano, D. Roccatano, Synthetic polymers and biomembranes. How do they interact Atomistic molecular dynamics simulation study of PEO in contact with a DMPC lipidbilayer,J.Phys. Chem. B 110 (2006) 26170-26179.

53. G. D'Errico, A. M. D'Ursi, D. Marsh, Interaction of a peptide derived from glycoprotein gp36 of feline immunodeficiency virus and its lipoylated analogue with phospholipidmembranes. Biochemistry47(2008)5317–5327.

54. E. K. Peter, I. V. Pivkin, A polarizable coarse-grained water model for dissipative particle dynamics, J. Chem. Phys. 141 (2014) 164506.

55. L. S. Romsted, Do amphiphile aggregate morphologies and interfacial compositions depend primarily on interfacial hydration and ion-specific interactions? The evidence from chemical trapping, Langmuir 23 (2007) 414–424.

56. L. Costantino, G. D'Errico, P. Roscigno, V. Vitagliano, Effect of urea and alkylureason micelle formation by a nonionic surfactant with short hydrophobic tail at 25 °C, J. Phys. Chem. B104 (2000) 7326–7333.

57. P. M. Kasson, E. Lindahl, V. S. Pande, Water ordering at membrane interfaces controls fusion dynamics, J. Am. Chem. Soc.133 (2011) 3812–3815.

$ %&' ( )* &#', - ./%&*/"

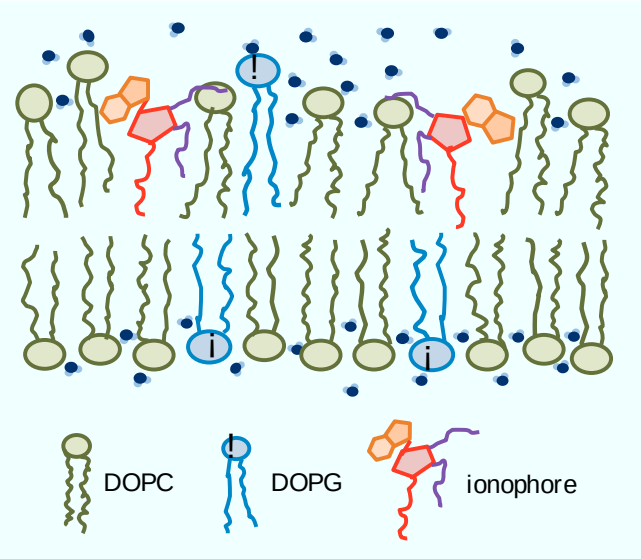
DOPC
DOPG
ionophore

"

"